Structure and morphology of Au grown on Ag(110)

P. Fenter and T. Gustafsson
Department of Physics and Astronomy and Laboratory for Surface Modification, P.O. Box 849, Rutgers—The State University of New Jersey, Piscataway, New Jersey 08855-0849
(Received 20 December 1990)

We report the results of an experimental investigation using medium-energy ion scattering of the growth of Au on the Ag(110) surface for Au coverages ranging from 0.05 up to 15 monolayers. The lattice parameters of Au and Ag are well matched, and the surface energies of Au and Ag are similar. One would therefore expect a simple growth mode [as earlier observed in the Au/Ag(111) system]. In contrast to this simple picture, we find the growth of Au/Ag(110) to be much more complex with several additional structural phenomena. At low Au coverages, the surface symmetry remains that of the (1×1) substrate. In the submonolayer coverage range, we find that Au grows in bilayer units in a Volmer-Weber growth mode. At higher coverages, the surface changes to a (1×3) and eventually to a (1×2) symmetry. With these changes of symmetry, we find changes in the growth properties such that the Ag surface is completely covered by the Au film in the (1×2) phase.

I. INTRODUCTION

The epitaxial growth of metals has been extensively studied over the past 50 years. The different possible growth modes are usually categorized in terms of the relative surface energies of the film-substrate combination.[1] Recently, it has been found in several systems that the growth does not fall within this classification scheme.[2–5] A detailed analysis of growth modes is important in understanding the basic structural properties of these surfaces, as well as in producing artificial nanoscale structures with interesting and possibly useful properties.

Epitaxial growth systems are traditionally classified based upon the change (Δ) in the surface free energy,[1] γ, when a substrate is covered with an overlayer material. For growth of Au on Ag, $\Delta=\gamma_{Au}-\gamma_{Ag}+\gamma_{int}$, where γ_{int} is the interface energy. If the system minimizes the surface free energy, then for $\Delta\leq 0$ layer by layer [Frank–van der Merwe (FM)] growth is expected, while for $\Delta\gg 0$, three-dimensional (3D) [Volmer-Weber (VW)] growth is expected. One can also argue that in highly strained systems with $\Delta<0$, the growth should follow the Stranski-Krastanov (SK) growth mode (with completion of the first layer followed by 3D growth in subsequent layers).

Based upon these considerations, the Au/Ag growth system is expected to be unusually simple. Since the surface energies of Au and Ag are similar[6] ($\gamma_{Au}=1.6$ J/m^2, $\gamma_{Ag}=1.3$ J/m^2) and the lattice constants of Au and Ag are essentially identical (4.08 versus 4.09 Å), the Au/Ag system should be an ideal growth system, unlike most other systems. Therefore, a layer-by-layer growth mode is expected. This has been directly observed in the Au/Ag(111) system,[7] and less direct evidence exists for layer-by-layer growth in the Au/Ag(100) system.[8]

The Au/Ag system has the interesting complication that all of the low index surfaces of Au reconstruct, while those of Ag do not. In particular, it is well known that the Au(110) surface reconstructs to a missing row structure with (1×2) symmetry.[9] Since the surface energy will change with the introduction of a surface reconstruction,[10] a reconstruction may have a strong impact upon the growth mode. Since the clean Ag(110) surface does not reconstruct and the growth parameters (surface energies and lattice constants) suggest layer-by-layer growth, it is an ideal template for studying the dependence of the Au surface reconstruction upon the Au crystal thickness. From this point of view, the simplest questions that can be asked are the following: (1) at what Au film thickness will the reconstruction appear and (2) how will the transformation from the nonreconstructed phase to the reconstructed phase take place? Both of these questions raise interesting issues concerning the nature of the reconstruction.

In a previous paper,[2] we have described the low-coverage growth of Au/Ag(110). We have shown that the initial growth of Au on Ag(110) occurs in bilayer units, and that these bilayer units grow in a Volmer-Weber growth mode. In this paper we provide an extensive description of our results for the low-coverage regime. In addition, we discuss the growth at higher Au coverages, where Au surface reconstructions appear and examine the effect of the surface reconstructions on the growth mode.

II. EXPERIMENT

A. Ion scattering and epitaxial growth

The experiments described below were performed using the technique of medium-energy ion scattering (MEIS) with channeling and blocking. The strength of ion scattering in this energy regime (50–400 keV) is that it is a truly quantitative structural probe, that is, the scattering cross sections are well known. The basic quantity measured is the number of backscattered ions (in ab-

solute units) as a function of energy and scattering angle (ϑ_s).

Our investigation of the growth mode with MEIS is based on two effects, shadowing and mass separation. When an ion beam scatters off an atom a shadow cone is formed.[11,12] For a static target atom, the shadow cone is a region where no ions can penetrate. Consequently, if the ion beam is aligned in such a way that the substrate atoms line up within this shadow cone, only the top layer atoms will be visible to the ion beam. Second, since Au is heavier than Ag, ions that scatter off Au will lose less energy than ions that scatter off Ag (see Fig. 1).[11,12] Accordingly, by measuring the energy of a scattered particle, one directly knows from which atom the ion has scattered. The combination of these two effects allows a direct measure of the growth mode of an overlayer film.

If, for example, the growth is epitaxial (that is, if the Au atoms sit in Ag lattice sites) then the Au overlayer atoms will shadow the Ag. Therefore, the Ag yield (that is, the number of ions that scatter off Ag atoms) should decrease in a linear fashion as Au is added. For a rigid lattice, each Au atom will cover completely one Ag atom; if thermal vibrations are taken into account, the Ag yield will decrease more slowly and even for a completely covered Ag substrate, the Ag yield may be finite. The rate of decrease of the Ag yield will contain information about the vibrational properties of the substrate and the adlayer. The shadowing, which is quite effective in the Au/Ag case due to the large nuclear charge of the Au atoms, should become even more effective when more than one Au layer is present. Furthermore, the rate at which the Ag yield decreases should change as an Au layer is completed. A plot of the substrate yield as a function of overlayer thickness will therefore show breaks when each successive layer is completed and growth in the next layer begins.[7]

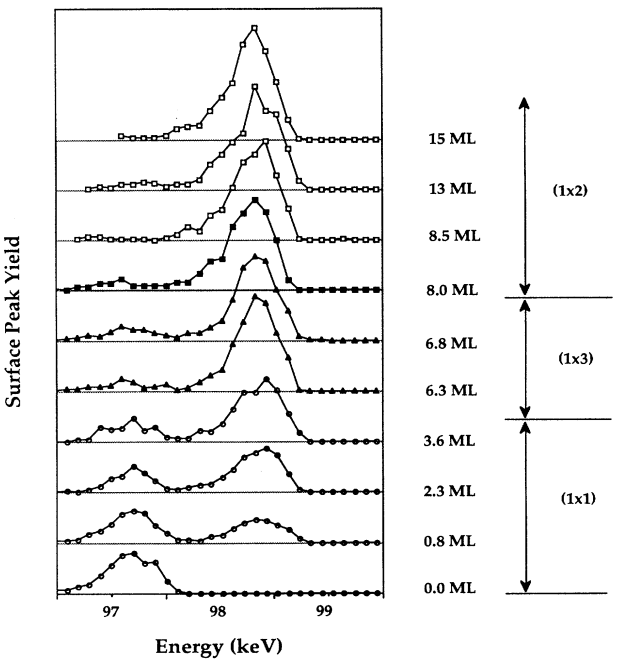

FIG. 1. The dependence of the surface peak yields (arbitrary units) and the surface symmetry on Au coverage. The higher (lower) energy peak is due to protons that have scattered off Au (Ag) atoms. Open circles correspond to (1×1) symmetry, while closed triangles and open squares correspond to (1×3) and (1×2) symmetries, respectively. The data shown as a crossed square displayed a poorly formed LEED pattern. Both the (1×1)→(1×3) and the (1×3)→(1×2) transitions are broad. The ion beam energy was 100 keV and the beam was incident normal to the Ag(110) substrate.

A second independent measure of the growth mode can be obtained by studying the scattering yield from the overlayer. It is convenient to define a quantity called $\chi_{\min}$, which is the ratio of the Au yield in a channeling direction to the Au yield in a nonchanneling (random incidence) direction.[7] Since all Au atoms are visible in a nonchanneling configuration, $\chi_{\min}$ is a measure of how many of the Au atoms are shadowed in a channeling configuration. For a flat uniform Au film of only one atomic layer, $\chi_{\min}=1.0$. At the point at which Au-Au shadowing takes place, $\chi_{\min}$ will drop below 1. Since different growth modes are distinguished by when second and higher layers begin to be occupied, $\chi_{\min}$ is a direct measure of the overall growth mode of the overlayer.

To understand the structure of the overlayer atoms in detail, we have studied the angular distribution of ions as they exit the crystal.[12] Ions that are scattered by overlayer atoms towards the detector may be prevented from exiting the crystal in certain directions. In these directions, called blocking directions, there is a reduction in the overlayer yield. The position and depth of the "blocking dips" then provide a simple and direct measure of the relative positions of the atoms in the overlayer, that is, the atomic morphology and structure. This type of analysis can be done with the ion beam in both channeling and nonchanneling directions. A comparison of the two will then provide further information on the morphology of the overlayer.

B. Sample preparation

The Ag(110) crystal was prepared and cleaned using standard surface-science procedures. The sample was sputtered with 0.5-keV Ne ions followed by a 2-min anneal at 425 °C before every Au deposition. The surface exhibited a well-defined (1×1) low-energy electron-diffraction (LEED) pattern, and showed no detectable impurities in Auger electron spectroscopy (AES) using a double-pass cylindrical-mirror analyzer. The incident protons were accelerated with a very stable 400-keV ion accelerator and the backscattered signal (number of ions versus angle) was measured with a high-resolution toroidal energy analyzer.[13] The Au films were grown at room temperature ($T<30$ °C) by evaporation from a W filament at a rate of roughly 1 monolayer (ML) per min (1.0 ML$=8.45\times10^{14}$ atoms/cm^2). The evaporation rate was varied by roughly a factor of 5 above and below this value and no changes were observed in the growth. Except where specified, the films were not annealed prior to measurement. The coverages quoted below were obtained directly from the ion beam signal and put on an

absolute scale by comparison with a calibrated standard[12]. Two different Ag crystals were used as substrates with essentially identical results.

III. RESULTS AND DISCUSSION

A. Epitaxy and the growth mode

Figure 1 shows the dependence of the surface peak yields on Au coverage for a normally incident ion beam. The clean Ag surface exhibits a clearly defined surface peak at an energy of 97.2 keV, while the Au surface peak appears at an energy of 98.4 keV. As Au is deposited, the size of this peak (i.e., the number of visible Ag atoms) decreases. This is due to Au-Ag shadowing, and shows that the growth is epitaxial. Because of the openness of the surface, 2 ML of Ag are completely visible to the ion beam in this geometry. If Au were growing in a layer-by-layer growth mode, the Ag yield should be greatly reduced for Au coverages above 2 ML. Since a large fraction of the Ag yield is visible even at $\Theta_{Au}=3.6$ ML, a layer-by-layer growth mode can be ruled out directly. Therefore, the Au is growing epitaxially, but in a Volmer-Weber growth mode.

By plotting the integrated area of the Ag surface peak as a function of Au coverage (Fig. 2) we can obtain more detailed information. Initially, the Ag yield exhibits a linear decrease with Au coverage. The decrease is due to Au atoms which shadow Ag atoms. This is therefore further evidence that Au grows epitaxially.[7] We also show a plot of χ_{min} for the Au overlayer as a function of coverage. Below $\Theta_c \approx 1$ ML, $\chi_{min}=1.0$, implying that all Au atoms arriving at the surface shadow only Ag atoms and no Au atoms. Because of the openness of the Ag(110) surface, there are 2 ML of Ag visible to the ion beam [see Fig. 2(a)]. Therefore, $\chi_{min} < 1.0$ only upon third-layer Au occupancy. If Au were growing in a FM mode, there should be no reduction in χ_{min} for coverages below 2.0 ML, at which point the Ag yield should be greatly reduced. This is clearly not the case, ruling out a FM growth mode. In addition, the linear reduction in the Ag yield implies that there is no disruption of the Ag substrate, and therefore no surface alloying or intermixing.

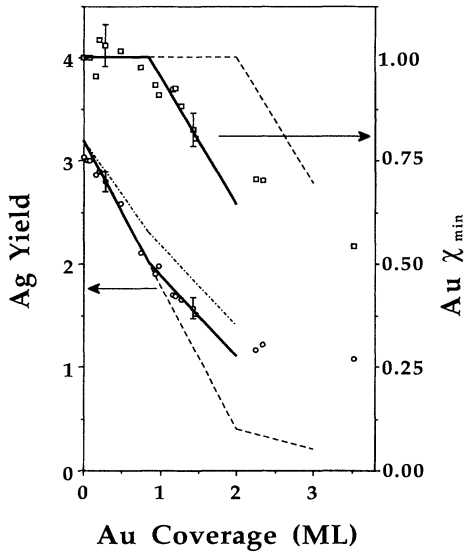

FIG. 2. Single alignment Ag yield in ML (circles) and Au χ_{min} (squares) plotted vs Au coverage for a 100-keV proton beam incident along $[\bar{1}\,\bar{0}0]$ and detected in the $(\bar{1}11)$ scattering plane at $\vartheta_s=130°$. The solid and dashed lines show what is expected for both the bilayer model (described in the text) and FM growth, respectively. The dashed-dotted line is also for the bilayer model, but for a larger surface vibrational amplitude. The break observed near 1 ML is due to third layer occupancy of Au atoms.

B. Low-coverage structure: Bilayers

In order to determine the structure of the Au layers below 1 ML we show both channeling and random incidence data (Fig. 3), taken in the $(\bar{1}11)$ scattering zone at a Au coverage of 0.22 ML. Both sets of data are characterized by a deep blocking dip. This dip is due to ions which scatter off Au atoms and then are blocked by other atoms before exciting the crystal. This directly implies that the Au structure consists of at *least* two atomic layers.

To investigate the possibility of having Au atoms present in more than two layers, we have taken data at random incidence. In random incidence [Fig. 3(c)], Au atoms in third or higher layers would *increase* the Au yield [dashed line in Fig. 3(d)], due to the absence of shadowing. There is no significant difference in the Au yield between the two sets of data. Therefore, the Au structure consists of *only* two layers. In addition, the yield at the blocking dip minimum is very close to *one-half* of the yield in the shoulders which directly implies that one-half

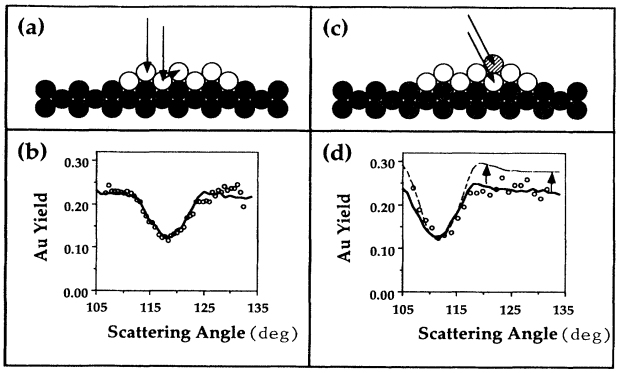

FIG. 3. (a) Side view of the crystal in the $(\bar{1}11)$ plane. Open (shaded) circles indicate Au (Ag) atoms. Arrows indicate the incident $[\bar{1}\,\bar{1}0]$ ion direction of the 100-keV incident protons. Note that one-half of the outgoing ions are blocked in the [101] blocking direction. (b) Au yield (ML) as a function of scattering angle (deg) for the geometry in (a). Circles are data points and the solid line is a Monte Carlo simulation for bilayer growth. (c) As in (a) but for ions incident 7° off the surface normal. (d) Au yield (ML) as a function of scattering angle for the geometry in (c). Note that if third or higher layers were present (cross-hatched circle) then the yield would increase away from the blocking direction (dashed line).

of the Au atoms occupy *second* layer sites.

The behavior observed in Fig. 3 is independent of the Au coverage in the submonolayer coverage regime. In Fig. 4(a) we show three data sets that range in coverage from 0.05 to 0.8 ML. Due to the large coverage difference it is difficult to directly compare them on one scale. Since the yield away from the blocking minimum corresponds to the Au coverage, we have divided out this dependence and show the yield on a coverage-independent scale [see Fig. 4(b)]. Clearly the data sets are identical within the (small) statistical deviations. We conclude that up to nearly 1 ML, Au grows epitaxially on Ag(110) in a *bilayer* form. For this to be possible the mobility of the Au atoms on the surface has to be quite high, but this is known to be the case.[7,14] Since 1 ML is the coverage corresponding to one Au atom per Ag (1×1) unit cell, at this coverage only one-half of the surface is covered with Au bilayers (presumably in islands).

The blocking dips shown in Figs. 2 and 3 are sensitive to both the detailed Au-Au spacing as well as the vibrational amplitude of the Au atoms. Somewhat simplified, the Au layer spacing can be directly determined from the data in Fig. 3 by using naive geometric arguments; that is, by assuming that the minimum of the surface blocking dip corresponds to the bond angle between the first- and second-layer Au atoms. If there were no relaxation, then the minimum would be at the bulk blocking direction of $\vartheta_s = 120°$. A *contraction* of the top layer would result in a shift to *smaller* scattering angles. In this simple picture, the relation between the scattering angle at the blocking dip minimum, $\vartheta_s^{\min}$, and the Au-Au relaxation, Δd_{Au}, is $\vartheta_s^{\min} = 90° + \tan^{-1}[(1-\Delta d_{\mathrm{Au}})/\sqrt{3})$. From the observed minimum at $\vartheta_s^{\min} \approx 118.5°$ it follows that $\Delta d_{\mathrm{Au}} \approx -6\%$. A detailed analysis of these data (and other data in this coverage range) based on Monte Carlo simulations (solid lines in Fig. 3) finds that the relaxation is $\Delta d_{\mathrm{Au}} = -6.3\pm0.3\%$, where the uncertainty in the relaxation reflects a statistical uncertainty from measurements at many Au coverages. This value can be compared to the theoretically predicted relaxation of a nonreconstructed Au surface[15] of $\Delta d_{12} = -9\%$. Although ours is not a semi-infinite Au(110)-(1×1) crystal, but only a two-layer-thick Au film, the two values agree very well, and can be contrasted with the relaxation of the clean (1×2) surface, $\Delta d_{12} = -18\%$.[10,16]

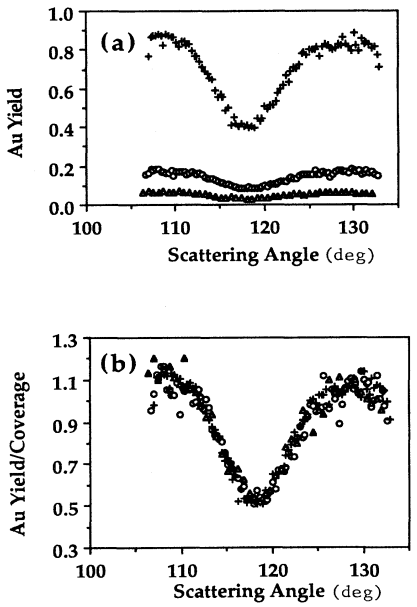

FIG. 4. (a) Au yield (ML) vs scattering angle (deg) for different Au coverages. Data taken in the same geometry and ion energy as in Fig. 2(b). (b) The data from (a) normalized to the Au coverage. Note that the data are identical to within statistical fluctuations.

Finite vibrational amplitudes make blocking less efficient and the surface blocking dip more shallow; that is, the yield at the surface blocking minimum increases. On the other hand, the yield away from blocking direction will be unaffected for this two-layer film since no blocking is taking place. Therefore, the depth of the dip is a direct measure of the vibrational amplitude. The surface vibrational amplitudes are generally not known; however, extensive modeling of MEIS data shows that the surface vibrational amplitudes (U_s) can be as much as a factor of 2 larger than the bulk values (U_b). The relationship between the size of the surface blocking dip and the vibrational amplitude can be quantified using Monte Carlo simulations for different vibrational amplitudes. We find an optimal agreement between the data in Fig. 3 and a simulation with $U_s/U_b = 1.0$; that is, we find the Au vibrational amplitude to be the same as the Au bulk vibrational amplitude.

A second independent measure of the Au vibrational amplitude is the change in the Ag yield as Au is deposited. To extract meaningful information, we must first understand the structure of the clean Ag(110) surface. Shown in Fig. 5 is the measured yield for normal incidence from the clean Ag(110) surface. Since there are no lateral distortions at the surface, the single alignment yield is determined *only* by the vibrational amplitude of the surface atoms. Given the surface vibrational amplitude, the relaxations are determined by the shift of the surface blocking minimum away from the bulk crystallographic direction. The solid line in Fig. 5(a) is a simulation of our best structural and vibrational parameters for these sets of data. This structure includes a contraction of the top layer spacing of $\Delta d_{12} = -10\%$, and an expansion of the second interlayer spacing of $\Delta d_{23} = +2\%$ (with respect to the bulk interlayer spacing of 1.45 Å). We also find a surface vibrational amplitude which is enhanced by a factor of 1.7 with respect to the bulk vibrational amplitude, slightly more than calculated by Jackson.[17] In comparing our structural values with other experiments (see Table I) we find very good agreement for Δd_{12} with a previous study of the Ag(110) surface using MEIS,[18] and reasonable agreement with earlier high-energy ion scattering[19] (HEIS) and LEED (Ref. 20) studies. A theoretical calculation[21] has predicted a first-layer contraction of $\Delta d_{12} = -7.4\%$. Our value for Δd_{23} is somewhat lower than earlier experimental values. Our surface vibrational enhancement is in reasonable agree-

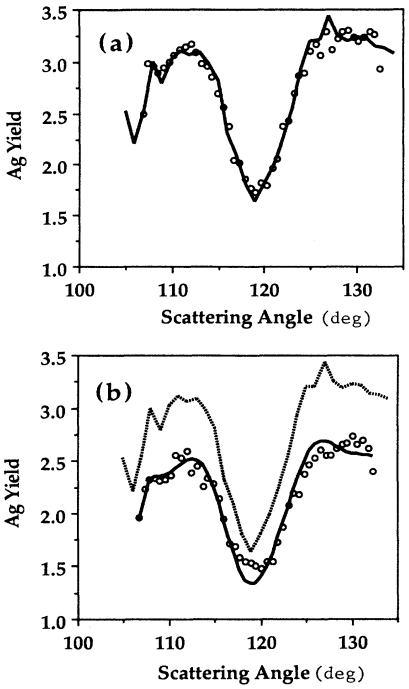

FIG. 5. Ag yield (ML) vs scattering angle (deg), taken in the same geometry and ion energy as in Fig. 2(b), for (a) the clean surface and (b) the surface with 0.44-ML Au adsorbed. The solid lines are simulations based upon the bilayer model (described in the text). The dashed line in (b) is the simulation for the clean surface shown in (a).

ment with earlier work.[18,19] It appears that our measured yields are somewhat lower than those reported in the earlier MEIS study,[18] but a detailed comparison is not possible as different scattering geometries were used.

As explained above, the initial slope of Y_{Ag} versus Θ_{Au} in Fig. 2 is a direct measure of the Au vibrational amplitude. This slope is consistent with the Au vibrational amplitude that we have found above (solid line in Fig. 2), although the determination is less accurate due to relatively fewer data points. The dashed-dotted line in Fig. 2 shows what is expected for a typical surface vibrational amplitude ($U_s \approx 2U_b$). The solid line clearly fits the data better, supporting the bulklike vibrational amplitude found above. In Fig. 5(b) we show the Ag blocking dip at a Au coverage of 0.44 ML. The whole angular distribution of the blocking dip is well described by the simulation that assumes the bilayer growth model for the Au atoms, and the clean Ag surface structure for the fraction of the Ag surface that is bare.

TABLE I. Structural parameters for Ag(110).

Technique	Δd_{12}	Δd_{23}
MEIS[a]	−10%	+2%
MEIS (Ref. 18)	−9%	+6%
LEED *I-V* (Ref. 20)	−7%	
HEIS (Ref. 19)	−7%	+4%
Theory (Ref. 21)	−7%	+2%

[a]Results of the present study.

To understand the vibrational amplitude that we have observed, it should be remembered that the Au atoms are now vibrating on a substrate of atoms with a lower mass. The Debye model predicts for this situation that for a given Debye temperature, the Au atoms will vibrate 30% less than the Ag atoms. Although this is somewhat smaller than the effect we observe, it may be an important contribution.

A second effect that must be taken into account in order to understand the vibrational amplitude is the correlation of the vibrational motion. Since the ion beam is only sensitive to relative displacements of atoms perpendicular to the ion beam, this effect must be included to convert the *measured* vibrational amplitude to an *absolute* vibrational amplitude. We do this by rescaling the vibrational amplitude U by a correlation coefficient[22] C, giving an effective vibrational amplitude of $U'=U\sqrt{1-C}$. C can be calculated in the Debye model, and for Au $C_D=0.37$. For Au, one can go one step further, as an analysis of the actual experimental bulk vibrational modes has been performed.[23] This has resulted in a correlation coefficient $C=0.3$. We have used the latter value in our analysis.

An alternative possible cause of the observed blocking effect in Fig. 3 must be considered: atomic mixing. Our data unambiguously show that Au is not growing in a simple one-layer structure, and (Fig. 3) that the Au atoms are located *only* in the top two layers of the crystal. The observed blocking dip is unambiguously due to ions that scatter off of Au atoms and are prevented from reaching the detector because they are blocked by other atoms in the crystal surface. It is conceivable that the blocking is due to Ag atoms; that is, the Au atoms have buried themselves in the Ag surface. Since the surface energies of Au and Ag are similar, there is no large energetic bias to force Au atoms into the Ag crystal. Nevertheless, it has been predicted that a concerted exchange diffusion mechanism[24] (which was originally proposed for bulk diffusion) exists on some surfaces even for the case of autoepitaxy[25] (where no energetic bias whatsoever exists). This type of spontaneous displacement of substrate atoms by adsorbate atoms has been experimentally observed in some metal-on-metal epitaxy systems, but ruled out in other systems.[25]

To model this situation we have included the possibility for a random mixing of the Au in the top two layers of the Ag crystal with a parameter, f_1 (f_2), which is the fraction of Au in the top (second) layer (such that $f_1+f_2=1.0$). To fit the observed behavior shown in Fig. 3, we have also varied the surface vibrational amplitude since both of these parameters effect the depth of the blocking dip. In Fig. 6 we show the range of the two parameters that will allow for a fit to the blocking data. For small vibrational amplitudes, we find $f_1 \approx 0.45$, while for large vibrational amplitudes $f_1 \approx 0$. This can be simply understood in that for larger vibrational amplitudes the blocking is much less efficient and therefore requires a greater fraction of the Au in the second layer. Therefore,

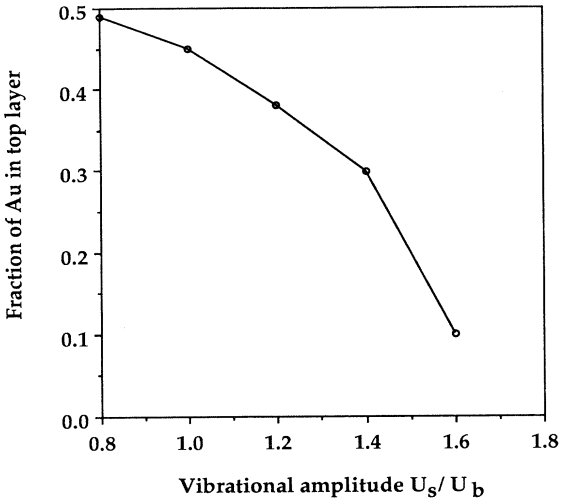

FIG. 6. The range of parameters (mixing fraction f_1 in the first layer vs surface vibrational amplitude U_s expressed in terms of the bulk vibrational amplitude U_b) that can fit the data in Fig. 2(b) in terms of an intermixing model.

to describe the blocking data, we must either assume that the Au is evenly mixed (with a small vibrational amplitude), or that the Au is located entirely in the second layer (for large vibrational amplitudes). From the blocking data alone, it is not possible to distinguish between these two possibilities. From the data in Fig. 2, we have measured the Au vibrational amplitude in a manner that was independent of the Au film structure. This analysis found a Au surface vibrational amplitude of $U_s = U_b$. Therefore, if mixing is present, it would require both an anomalously small surface vibrational amplitude, and a mixing of $f_1 \approx 0.45$.

A second piece of evidence that the Au layers consist of two equally populated layers comes from the shape of the Au surface peak (Fig. 7). Since ions lose energy at a constant rate in solids, dE/dx, due to collisions with electrons, the energy scale of the surface peak can be converted to a depth scale.[11] Consequently, the shape of the surface peak is sensitive to the arrangement of the Au atoms. We have measured the resolution function of the ion energy analyzer by passing the ion beam from the accelerator *directly* through the analyzer. We find that the resolution function can be fit by a single Gaussian with a full width at half maximum (FWHM) of 405 eV [Fig. 7(a)]. The fit is satisfactory except in the tails of the distribution where the Gaussian function is too broad. The surface peak for 100-keV protons scattered off a 0.73-ML Au film at a scattering angle of 127° is shown in Fig. 7(b). The solid line is a fit to these data with the known resolution function of the analyzer assuming a single layer of Au. The surface peak is significantly wider than the calculation implying that more than one layer is involved. The bilayer structure is a natural way of introducing two contributions into the surface peak. With hitting probabilities from the Monte Carlo simulations for a Au bilayer at this scattering angle, and a rate of energy loss of

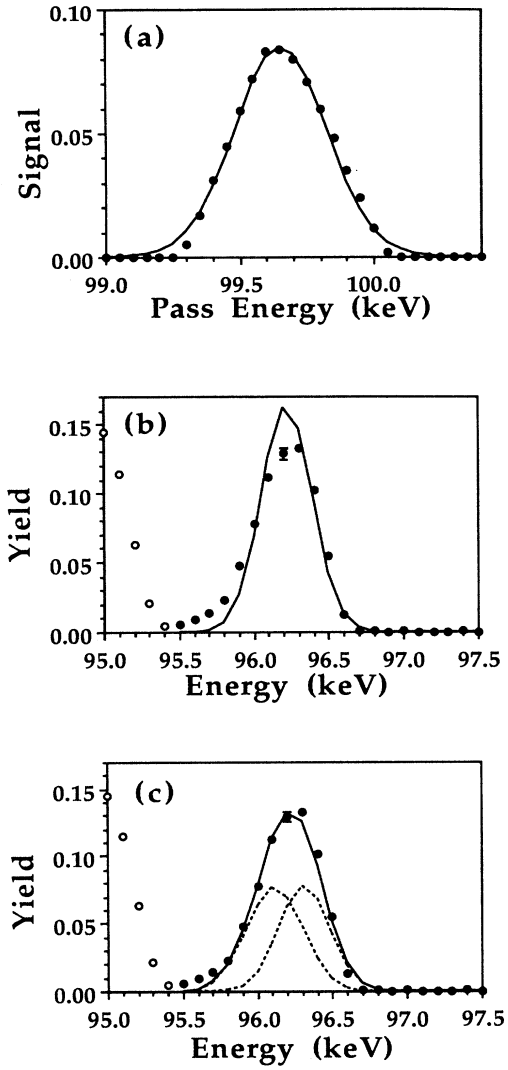

FIG. 7. (a) The measured resolution function of the electrostatic energy analyzer for a 100-keV proton beam and a fit to this function using a Gaussian with a width of 405 eV. (b) The Au surface peak from 100-keV protons scattered off a 0.73-ML Au film (solid points) and a fit to this peak with contributions from a single Au layer. (c) The same data as in (b) fitted with two successive layers using a rate of energy loss of 53 eV/Å. The Ag yield is shown with open circles and was not included in the fitting procedure.

$dE/dx = 53$ eV/Å, the surface peak shape can be reproduced accurately [Fig. 7(c)] over the full range of the data. (It should be noted that the mean energy loss for protons in Au is known to be 23 eV/Å,[26] but that in channeling configurations, the rate can be much higher,[27,28] consistent with our results.)

Based upon these data, it is possible to say that the Au layers consist of two atomic layers with an equal fraction of Au in each layer. Therefore, of the two possible models that can explain the observed behavior, the bilayer model appears to be the most consistent. It involves

fewer parameters and its only unusual feature, the value of the vibrational amplitude, is shared by the mixing model.

At coverages above 1 ML (Fig. 2), $\chi_{\min}$ decreases, directly implying that third- (or higher-) layer sites are being occupied. Since we have shown that Au is growing in bilayers, for a complete bilayer the break should occur at 2 ML; that the break occurs at a lower coverage means that the surface is not completely covered at this point. This may be due to microscopic imperfections on the crystal preventing continued 2D growth. Therefore, Au is growing in a bilayer VW growth mode (3D islanding before covering the substrate). The information from the blocking curves was essential in reaching this conclusion; from the data in Fig. 2 only, one might simply assume that the Au had completed the first monolayer and continued to grow in 3D clusters above Θ_c (i.e., a Stranski-Krastanov mode).

C. Intermediate coverages

Although the LEED pattern does not change as the Au coverage is increased above 1 ML, the growth properties of the Au films begin to change. We have previously described this coverage regime,[2] and therefore we will only briefly outline the results here for completeness. Above Au coverages of 1 ML (where the substrate is only half covered by the Au film), we can directly see that the Au begins to grow in a 3D fashion. By analyzing ion scattering data at a variety of incident directions, we were able to get direct information on the morphology of the film as it begins to grow in 3D clusters. For example, the resulting picture for a Au coverage of 1.4 ML is that the morphology of the Au film is such that the first two Au layers contain equal Au coverages ($\Theta_{1,2}=0.55$ ML) and, in addition, the third and fourth layers also contain equal Au coverages ($\Theta_{3,4}=0.15$ ML), while we do not detect any fifth-layer occupancy at all. That is, the initial 3D growth also occurs in a bilayer structure.[2]

D. Higher-coverage growth: Reconstruction and wetting

For the first few monolayers, the symmetry of the Au films does not change from the (1×1) symmetry of the clean Ag(110) substrate. Eventually, the Au films should exhibit the (1×2) symmetry of the Au(110) surface. The relevant questions are then the following: how and when does this transition occur? One simple expectation is that at some critical coverage, the Au reconstruction will become energetically favorable, and after adding 0.5 ML of Au atoms, the reconstruction will be fully formed.

In Fig. 1 we show the changes of symmetry of the surface as the Au coverage is increased in the multilayer range. At the highest coverages, the Au overlayers acquire the expected (1×2) symmetry for the missing row reconstruction. But surprisingly, the Au films exhibit a (1×3) symmetry at coverages intermediate between the (1×1) and (1×2) structures. In addition, the LEED pattern becomes poorly formed both above and below the (1×3) phase. This indicates that disordering is taking place, and that the different phases do not coexist on the surface over microscopically large regions.

In addition to the changes of symmetry, the growth behavior of the Au films changes as well. In the (1×1) phase, a large fraction of the Ag yield observed for the clean surface is always visible to the ion beam (see Fig. 1), implying that the Au is not wetting the Ag substrate. This is consistent with the earlier description of the 3D growth above 1 ML coverages.[2] When the symmetry of the surface is converted to (1×3), it can be seen that while the Ag yield is reduced to about 0.6 ML, it is still far from zero. Therefore, Au is nearly covering the substrate but areas of bare Ag persist. As more Au is added to the (1×3) phase, the amount of visible Ag does not change appreciably. It is not until the (1×2) phase is formed that the Ag yield vanishes. This is a clear sign that the Au completely covers the Ag substrate. Since wetting requires that the surface free energy of the film-substrate combination is lowered with respect to the clean surface,[1] that is, $\Delta=\gamma_{\mathrm{Au}}-\gamma_{\mathrm{Ag}}+\gamma_{\mathrm{int}}<0$, our observations imply that the surface free energy of the (1×2) phase satisfies this condition while the surface free energies of the (1×1) and (1×3) phases do not; that is, *the wetting has been induced by the surface energy reduction due to the introduction of the reconstruction.*

More information on the relative energetics of these phases can be found by gently annealing the overlayer film. We have found that the (1×2) phase is stable to a short anneal at 100 °C, while both the (1×3) and (1×1) phases are unstable. Since the wetting of the (1×2) phase is due to the lowering of the total energy, this phase is expected to be stable. Similarly, the (1×3) and (1×1) phases are not expected to be thermally stable since its total energy can be lowered by reducing the total area of the Au film surface. Therefore, both the (1×3) and (1×1) films are only metastable.

A second interpretation of the data in Fig. 8 is that the Au is covering the Ag substrate uniformly, but that there is a certain amount of Ag that is acting as a surfactant,[29]

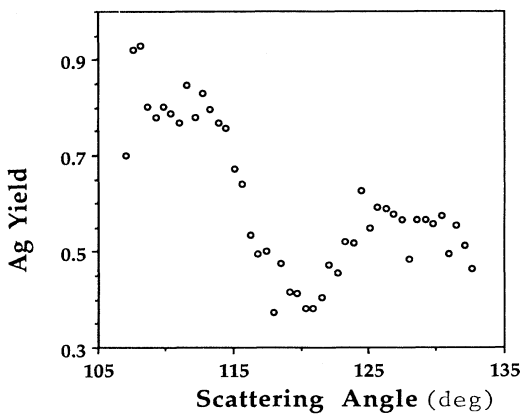

FIG. 8. The Ag yield (ML) vs scattering angle (deg) in the (1×3) phase (Au coverage $=6.3$ ML). Note the deep blocking dip which rules out a simple surfactant model. (The asymmetry of the dip is due to overlap with the Au yield at smaller scattering angles.)

and is continually rising to the surface as Au is added. This model is appealing since the addition of Ag to Au(110) can produce a (1×3) structure,[30] although this transition requires the substrate to be annealed. In addition, this would support the idea that the Au atoms initially mix with the Ag substrate at low coverages. In this case one would expect that the Ag would only occupy sites in the top of the surface, since Ag atoms in second and deeper layers would not be capable of exchanging with a surface Au atom and would quickly get buried. In contrast to this, the angular distribution of ions scattered off Ag at these coverages show a deep blocking dip (Fig. 8) which does not change significantly with Au coverage. This directly shows that the Ag is not present only in the top layer. Consequently, the surfactant model (and therefore the mixing model for initial growth) is not supported by the data.

In principle, the (1×1) to (1×2) transition should require (at most) the addition of 0.5 ML of Au, which is the difference in surface density of the (1×1) and (1×2) phases (see Fig. 9). Since we are adding Au atoms to the surface, mass transfer should not be the limiting factor in this transition. In contrast, we find that an additional ~4 ML of Au is needed to complete the (1×1) to (1×2) transition. Therefore, it is likely that the (1×3) phase has a lower surface energy than the (1×1) phase. This is consistent with the observation that more of the substrate is covered by the (1×3) phase than the (1×1) phase, and the wetting condition is closer to being satisfied. Therefore, it is possible to say that $\gamma_{(1\times2)} < \gamma_{(1\times3)} < \gamma_{(1\times1)}$.

Although the (1×2) phase is clearly the missing row reconstruction, the structure of the (1×3) phase is not yet known. It is interesting to note that the addition of alkali atoms to the Ag(110) surface [and other fcc (110) surfaces] results in a (1×2) missing row reconstruction, and that a (1×3) phase is observed as an intermediate state.[31] Since mass transfer is necessary in the alkali-induced structural transition, it is not as clear whether this (1×3) phase is due solely to the limitations of mass transfer or if it is an energetically favored structure. In the analogous growth system of Pt/Pd(110), a (1×3) phase is also observed as an intermediate phase between the (1×1) and (1×2), although many details of the growth are different.[32] Since the intermediate (1×3) is prevalent in the conversion of a nonreconstructed surface to a missing row reconstruction[31] and vice versa,[30] it is likely that it is a general characteristic of this transition, and is therefore of interest to know its structure. Although we have taken blocking spectra of the (1×3) phase they are not a good test of the different structural models since the Au films did not yet cover the Ag surface. Therefore, these spectra are sensitive to not only the Au structure, but the morphology of the films and especially the fraction of the surface that is covered. This dependence on multiple parameters means that the absolute scattering yield constrains the purely structural parameters less, and makes structural analysis difficult. But information on the structure of the (1×3) phase can be inferred from other experimental evidence.

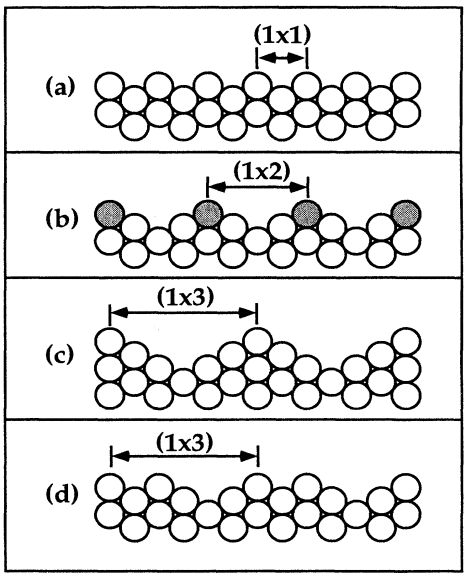

FIG. 9. A schematic of the relevant reconstructions of Au surfaces, including (a) the (1×1) nonreconstructed surface, (b) the (1×2) missing row reconstruction, (c) the (1×3) generalized missing row reconstruction, and (d) the (1×3) mixed structure.

A (1×3) structure that is known to exist is the "generalized" missing row reconstruction that has been observed on the Au(110) (Refs. 33 and 34) and Pt(110) (Ref. 35) surfaces as shown in Fig. 9(c). This structure has the feature that large (111) facets are exposed. This structure also has the interesting property that it has the same surface density as the nonreconstructed surface; that is, no mass transfer is needed between these two structures. Therefore, it would be expected that in a transformation from the nonreconstructed surface to the missing row structure, the (1×1)→(1×3) transition would be quick (requiring no change in the surface density), while the (1×3)→(1×2) transition would be slow (requiring 0.5 ML change in the surface density). In contrast the (1×1)→(1×3) is as slow as the (1×3)→(1×2) transition. This simple analysis therefore suggests that the (1×3) phase does not correspond to a generalized missing row structure. Since the (1×3) phase can be formed with the addition of only 0.05 ML of alkali atoms to the Au(110)-(1×2) surface,[34] one can infer that the surface energies of these two phases are very similar. Theoretical calculations support this idea.[36,37] The changes in the growth behavior that we have observed imply that there is a significant difference in the surface energies of the (1×3) and (1×2) phases observed in the Au/Ag case. This also implies that the generalized missing row reconstruction does not explain the observed behavior.

A structure that may explain the observed behavior is shown in Fig. 9(d). This structure is a mixture of (1×1) and (1×2) unit cells. Since the structure of this phase is significantly different than either the (1×1) or (1×2) phases, its surface energy should also differ significantly, explaining the growth behavior. Of course, this conclusion is only tentative until a detailed structural analysis is performed.

IV. CONCLUSIONS

We have studied the morphology and structure of ultrathin Au films grown on Ag(110). These films have demonstrated interesting growth behavior as a function of Au coverage. Initially, the overall growth has been found to be a Volmer-Weber (3D) growth mode. This can be understood on energetic grounds if the change in the surface free energy, $\Delta=\gamma_{Au}-\gamma_{Ag}+\gamma_{int}$, of the Au/Ag system is positive. Although simple theoretical estimates find $\Delta\approx+0.3$ J/m^2, this is probably not large enough to induce a VW growth mode as evidenced by the FM (layer-by-layer) growth mode that is observed on the (111) (Ref. 7) and (100) (Ref. 8) surfaces of Ag. It is likely that the surface orientation [and perhaps the preference of the (110) surface to reconstruct] may have changed the surface energy of the Au film sufficiently so that a VW growth mode is preferred.

At higher coverages we have found that the growth mode changes, and that these changes are correlated with the surface reconstructions that appear. As more Au is added, the surface energy is lowered and the fraction of the Ag substrate that is covered increases until the (1×2) phase appears at which point the Au completely wets the surface. These changes can be understood in that the surface energy of the Au is decreasing as each reconstruction appears. When the (1×2) phase is formed the Au surface energy is low enough to satisfy the wetting condition ($\Delta<0$).

Although the Au *film* is not stable until the (1×2) reconstruction is fully formed, the surface structures appear to be energetically favorable. Since Au atoms are known to be mobile,[7,14] as they are added they should arrange themselves in an energetically favorable configuration. Since we have observed the surface symmetry to change as a function of Au coverage, these changes should reflect the energetics of these reconstructions as a function of Au thickness, *independent* of the film energetics. Therefore, the (1×3) phase may be a common characteristic of the $(1\times1)\rightarrow(1\times2)$ transition.

Although it is straightforward to understand the overall growth mode, it is difficult to understand the bilayer growth in detail. In the case of semiconductor surfaces, growth is known to take place in double layers,[38] but this is intimately connected with the lattice structure. Although the Ag(110) surface consists of double layers (for translational invariance along the [110] direction), each layer is equivalent and it is therefore difficult to understand why Au atoms introduced to the surface would prefer to bond in only such a structure. Other reports of bilayer growth have appeared recently in metal-on-metal epitaxy. Most intriguing is the report that the Pb/Cu(111) system grows in both bilayers and single layers with a seemingly random sequence.[3] This has been explained in terms of a layer-dependent surface energy (quantum size effect), with the layer sequence being determined by "magic" thicknesses (integer multiples of half the Fermi wavelength) as suggested by some calculations.[39,40] The Co/Cu(100) system has also very recently been found to be a bilayer growth mode.[4] In this case, since the surface energy of Co is expected to be much higher than Cu,[6,41] nonideal growth modes might be expected.

A simple explanation for the bilayer growth that we have observed is that it may be due to the presence of steps on the Ag(110) surface. This can also explain how it was possible to observe bilayer growth down to a coverage of 0.05 ML in Fig. 4. If the Au films were to nucleate randomly on the surface, edge effects (which would show up as a decrease of the *depth* of the blocking dip) should be seen at these coverages. Conversely, steps provide nucleation sites for the Au atoms, and since they are known to be mobile at room temperature, relatively large islands can appear (>50 Å) without difficulty. That we see bilayer growth instead of single-layer growth may be an indication that Au prefers to bond to double height steps.

In conclusion, we have found that Au grows epitaxially on Ag(110), and that for the first few monolayers, the Au films do not show any evidence of the (1×2) reconstruction which is present on the semi-infinite Au(110) crystal surface. In addition, our data demonstrate that Au initially prefers to grow in a bilayer VW growth mode on Ag(110). This growth mode is not predicted by simple energetic considerations. At high coverages, surface reconstructions appear which induce the Au films to wet the surface.

ACKNOWLEDGMENTS

We would like to thank M. Chester for his help and many valuable discussions and Dr. D. M. Zehner for lending us the Ag(110) substrate. This research was supported by NSF Grants No. DMR-8703897 and No. DMR-9019868.

[1]E. Bauer, Appl. Surf. Sci. **11/12**, 479 (1982).
[2]P. Fenter and T. Gustafsson, Phys. Rev. Lett. **64**, 1142 (1990).
[3]B. J. Hinch, C. Koziol, J. P. Toennies, and G. Zhang, Europhys. Lett. **10**, 341 (1989).
[4]Hong Li and B. P. Tonner, Surf. Sci. **237**, 141 (1990).
[5]P. J. Schmitz, W.-Y. Leung, G. W. Graham, and P. A. Thiel, Phys. Rev. B **40**, 11 477 (1989).
[6]L. Z. Mezey and J. Giber, Jpn. J. Appl. Phys. **21**, 1569 (1982).
[7]R. J. Culbertson, L. C. Feldman, P. J. Silverman, and H. Boehm, Phys. Rev. Lett. **47**, 657 (1981).
[8]T. C. Hsieh, A. P. Shapiro, and T.-C. Chiang, Phys. Rev. B **31**, 2541 (1985).
[9]W. Moritz and D. Wolf, Surf. Sci. **163**, L655 (1985).
[10]K.-M. Ho and K. P. Bohnen, Phys. Rev. Lett. **59**, 1833 (1987).
[11]L. C. Feldman, J. W. Mayer, and S. T. Picraux, *Materials Analysis by Ion Channeling* (Academic, New York, 1982).
[12]J. F. van der Veen, Surf. Sci. Rep. **5**, 199 (1985).
[13]High Voltage Engineering Europa, Amersfoort, The Netherlands.
[14]R. C. Jaklevic and L. Elie, Phys. Rev. Lett. **60**, 120 (1988).

[15]K.-M. Ho and K. P. Bohnen, Europhys. Lett. **4**, 345 (1987).
[16]M. Copel and T. Gustafsson, Phys. Rev. Lett. **57**, 723 (1986).
[17]D. P. Jackson, Surf. Sci. **43**, 431 (1974).
[18]E. Holub-Krappe, K. Horn, J. W. M. Frenken, R. L. Krans, and J. F. van der Veen, Surf. Sci. **188**, 335 (1987).
[19]Y. Kuk and L. C. Feldman, Phys. Rev. Lett. **30**, 5811 (1984).
[20]E. Zanazzi, F. Jona, D. W. Jepsen, and P. M. Marcus, J. Phys. C **10**, 375 (1977).
[21]C. L. Fu and K. M. Ho, Phys. Rev. Lett. **63**, 1617 (1989).
[22]D. P. Jackson, T. E. Jackman, J. A. Davies, W. A. Unertl, and P. D. Norton, Surf. Sci. **126**, 226 (1983).
[23]S. P. Withrow, J. H. Barrett, and R. J. Culbertson, Surf. Sci. **161**, 596 (1985).
[24]K. C. Pandey, Phys. Rev. Lett. **57**, 2287 (1986).
[25]P. J. Feibelman and G. L. Kellogg (unpublished).
[26]J. F. Ziegler, J. P. Beiersack, and U. Littmark, *The Stopping and Ranges of Ions in Matter* (Pergamon, New York, 1985), Vol. 3.
[27]P. Statiris, P. Fenter, and T. Gustafsson (unpublished).
[28]P. F. A. Alkemade, W. C. Turkenburg, and W. F. van der Weg, Nucl. Instrum. Methods B **28**, 161 (1987).
[29]M. Copel, M. C. Reuter, Efthimios Kaxiras, and R. M. Tromp, Phys. Rev. Lett. **63**, 632 (1989).
[30]A. Morgante, K. C. Prince, G. Paolucci, and E. Tosatti, Surf. Sci. **189/190**, 620 (1987).
[31]B. E. Hayden, K. C. Prince, P. J. Davie, G. Paolucci, and A. M. Bradshaw, Solid State Commun. **48**, 325 (1983).
[32]W.-Y. Leung, P. J. Schmitz, and P. A. Theil, Bull. Am. Phys. Soc. **34**, 578 (1989).
[33]G. A. Held, J. L. Jordan-Sweet, P. M. Horn, A. Mak, and R. J. Birgeneau, Solid State Commun. **72**, 37 (1989).
[34]P. Häberle, P. Fenter, and T. Gustafsson, Phys. Rev. B **39**, 5810 (1989).
[35]P. Fery, W. Moritz, and D. Wolf, Phys. Rev. B **38**, 7275 (1988).
[36]S. M. Foiles, Surf. Sci. **191**, L779 (1987).
[37]M. Garofalo, E. Tosatti, and F. Ercolessi, Surf. Sci. **188**, 321 (1987).
[38]E. Vlieg, A. W. Denier van der Gon, J. F. van der Veen, J. E. Macdonald, and C. Norris, Phys. Rev. Lett. **61**, 2241 (1988).
[39]P. J. Feibelman, Phys. Rev. B **27**, 1991 (1983).
[40]K. F. Schulte, Surf. Sci. **55**, 427 (1976).
[41]W. R. Tyson and W. A. Miller, Surf. Sci. **62**, 267 (1977).